J Shoulder Elbow Surg (2020) 29, 1450–1459

ELSEVIER

Journal of Shoulder and Elbow Surgery

www.elsevier.com/locate/ymse

Vault perforation after eccentric glenoid reaming for deformity correction in anatomic total shoulder arthroplasty

Adam Olszewski, BS, ATC[a,1], Austin J. Ramme, MD, PhD[a,1], Tristan Maerz, PhD[a], Michael T. Freehill, MD[a], Jon J.P. Warner, MD[b], Asheesh Bedi, MD[a,*]

[a]*Department of Orthopaedic Surgery, University of Michigan, Ann Arbor, MI, USA*
[b]*Boston Shoulder Institute, Massachusetts General Hospital, Boston, MA, USA*

Background: The management of glenoid deformity during anatomic total shoulder arthroplasty remains controversial. In this study, we evaluate variable correction of glenoid deformity by eccentric reaming. We hypothesize that partial correction of modified Walch B/C-type glenoid deformities can achieve 75% bone-implant contact area (BICA) with a reduced vault perforation risk compared with complete correction.
Methods: Fifty shoulder computed tomographic scans with glenohumeral osteoarthritis were retrospectively evaluated. The Tornier BluePrint v2.1.5 software simulated 3 eccentric reaming scenarios including no, partial, and complete deformity correction. Each scenario was evaluated at 4 BICAs and using 3 implant fixation types. Three-dimensional surface representations were used to evaluate medialization and vault perforation.
Results: The patients had mean glenoid retroversion and inclination of 18.5° and 8.8°, respectively, and mean posterior humeral head subluxation of 76%. With 75% BICA, the 3 fixation types had glenoid vault perforation in 6%-26% and 26%-54% of cases for partial and complete glenoid deformity correction, respectively. The central and posterior-inferior implant components were most likely to perforate across all scenarios.
Discussion: Eccentric reaming for glenoid deformity correction increases the risk of vault perforation. Severe glenoid deformity required increased medialization to achieve 75% BICA. Pegged implants have increased chances of perforation compared with a keeled design; the central and posterior-inferior components were most likely to perforate during deformity correction.
Conclusion: Partial deformity correction of modified Walch B/C-type glenoid deformities can achieve 75% BICA while reducing the risk of vault perforation compared with complete correction at the time of anatomic total shoulder arthroplasty.
Level of evidence: Basic Science Study; Computer Modeling

Keywords: 3D surgical simulation; surgical planning; glenoid bone stock; arthroplasty templating; implant perforation; implant contact area

The University of Michigan Institutional Review Board approved this study (HUM00130515).

[1] These authors contributed equally to this work.

*Reprint requests: Asheesh Bedi, MD, Department of Orthopaedic Surgery, University of Michigan, 24 Frank Lloyd Wright Drive, Lobby A, P.O. Box 391, Ann Arbor, MI 48106, USA.
E-mail address: abedi@med.umich.edu (A. Bedi).

1058-2746/$ - see front matter
https://doi.org/10.1016/j.jse.2019.11.011

Modern 3-dimensional surgical software is rapidly becoming available for preoperative planning of orthopedic surgical cases, including deformity correction, arthroplasty, and fracture management. Various software platforms allow radiographs, computed tomography (CT), and magnetic resonance imaging to be useful for preoperative planning.[6-9,12,18,34,36,37,39,52] Preoperative templating can help to prevent intraoperative fracture, decrease overall surgical time, and reduce the number of case-specific surgical trays.[38]

In anatomic total shoulder arthroplasty (TSA), 3-dimensional planning allows for optimization of implant sizing, orientation, and positioning prior to entering the operating room. Especially in the cases of complex and atypical glenoid morphology, preoperative planning helps to achieve a stable construct and reduce the risk of glenoid vault perforation.[4,9,12,19,22,32,47,49,52] Suboptimal implant positioning increases the risk of revision surgery and can cause reduced outcome scores.[9,12,33,44]

Failure to correct retroverted glenoid deformity increases the risk of glenoid component loosening and failure.[17] Farron et al[11] demonstrated by finite element analysis that more than 10° of glenoid implant retroversion is a risk factor for component loosening. One method of glenoid deformity correction is eccentric reaming; however, the amount of medialization during eccentric reaming is limited by glenoid bone stock and the risk of implant perforation. Implant perforation may predispose the component to loosening and should be avoided whenever possible.[14,32,40] It has been recommended that eccentric reaming be considered to correct up to 10°-15° of glenoid retroversion in cases that have less than 80% posterior humeral subluxation.[23,43,46,48] Other options to address complex glenoid deformity include augmented glenoid implant designs,[13,15,41] bone grafting,[5,10,24,27] and conversion to a reverse total shoulder implant system.[30,31]

The appropriate management of the complex and eccentrically worn glenoid deformity (modified Walch B/C-type) in anatomic TSA remains controversial.[15,50] In this study, we have performed a thorough evaluation of the effect of eccentric reaming for complex glenoid deformity correction on vault perforation with pegged, keel, and hybrid glenoid component designs. We hypothesize that partial correction of retroversion through eccentric reaming may allow for adequate bone-implant contact area (BICA) for stable implantation and reduced risk of vault perforation. Furthermore, we hypothesized that a keeled implant design would offer a reduced risk of vault perforation for all degrees of correction of complex glenoid deformity.

Materials and methods

After institutional review board approval, 50 CT scans were retrospectively evaluated from 2 institutions. Inclusion criterion was primary glenohumeral osteoarthritis in patients who have undergone an anatomic TSA by one of 2 senior authors between January 1, 2010, and May 1, 2017. Glenoids were graded using the modified Walch classification by 3 orthopedic surgeons, and if any disagreement occurred, then consensus was used.[3] Exclusion criteria were inflammatory arthritis, rotator cuff arthropathy, and modified Walch A-type glenoids.

The Tornier BluePrint v2.1.5 software was used to simulate glenoid deformity correction by eccentric reaming. The software uses a 3D surface-based measurement method to determine the retroversion, inclination, and posterior humeral head subluxation values. This method involves automated 3D segmentation of the CT images to establish a point cloud–based triangulated surface rendering of the scapula and humeral head. A 3D coordinate system for the scapula is based on a best-fit plane to the scapula and on an axis defined by the intersection of the scapular spine and scapular body. The glenoid fossa point-cloud is used to calculate a glenoid centerpoint. This centerpoint determines the origin of the coordinate system for the previously defined scapular axes. A best-fit sphere is calculated to fit into the glenoid fossa. The best-fit sphere centerpoint and the glenoid fossa centerpoint are used to determine the glenoid retroversion and inclination based on the 3D scapular coordinate system. The previously generated humeral head point-cloud is used to calculate the proportion of the humeral head that falls posterior to the centerpoint of the glenoid fossa. This value is used to calculate the percentage of posterior humeral head subluxation.

The BluePrint software incorporates the Wright Tornier Aequalis Perform Glenoid System (Bloomington, MN, USA) including Cortiloc, pegged, and keeled glenoid components (Fig. 1). We simulated 3 glenoid deformity correction scenarios: scenario 1, no deformity correction; scenario 2, partial deformity correction to neutral inclination and 10° retroversion; and scenario 3, complete deformity correction to neutral inclination and version. Each deformity correction scenario was evaluated at 4 implant-bone contact percentages (25%, 50%, 75%, 95%) and using each of 3 implant fixation types. Three-dimensional surface representations of each patient were used to evaluate medialization distance and location of glenoid vault perforation (Fig. 2). Color-coded BICA maps were generated using the Tornier BluePrint software for each simulation to visualize contact patterns (Fig. 3) based on glenoid deformity correction. Standard descriptive statistics were used to evaluate the risk of perforation in each scenario.

Results

A total of 1800 3D surgical simulations of glenoid implant deformity correction were performed (50 subjects, 3 deformity correction simulations, 4 BICAs, and 3 implant fixation types). The 50 subjects (mean age 66 years; sex, 48% female) included Walch grades B1 (n = 4), B2 (n = 29), B3 (n = 13), and C (n = 4), with a mean retroversion of 18.5° (standard deviation 7.0°), mean inclination of 8.8° (standard deviation 7.4°), and mean posterior humeral head subluxation of 76% (standard deviation 10%). The amount of medialization required for glenoid version and inclination correction was similar among all implant fixation types: Cortiloc (Table I), pegged (Table II), and keeled (Table III). Across all subjects, the mean medialization

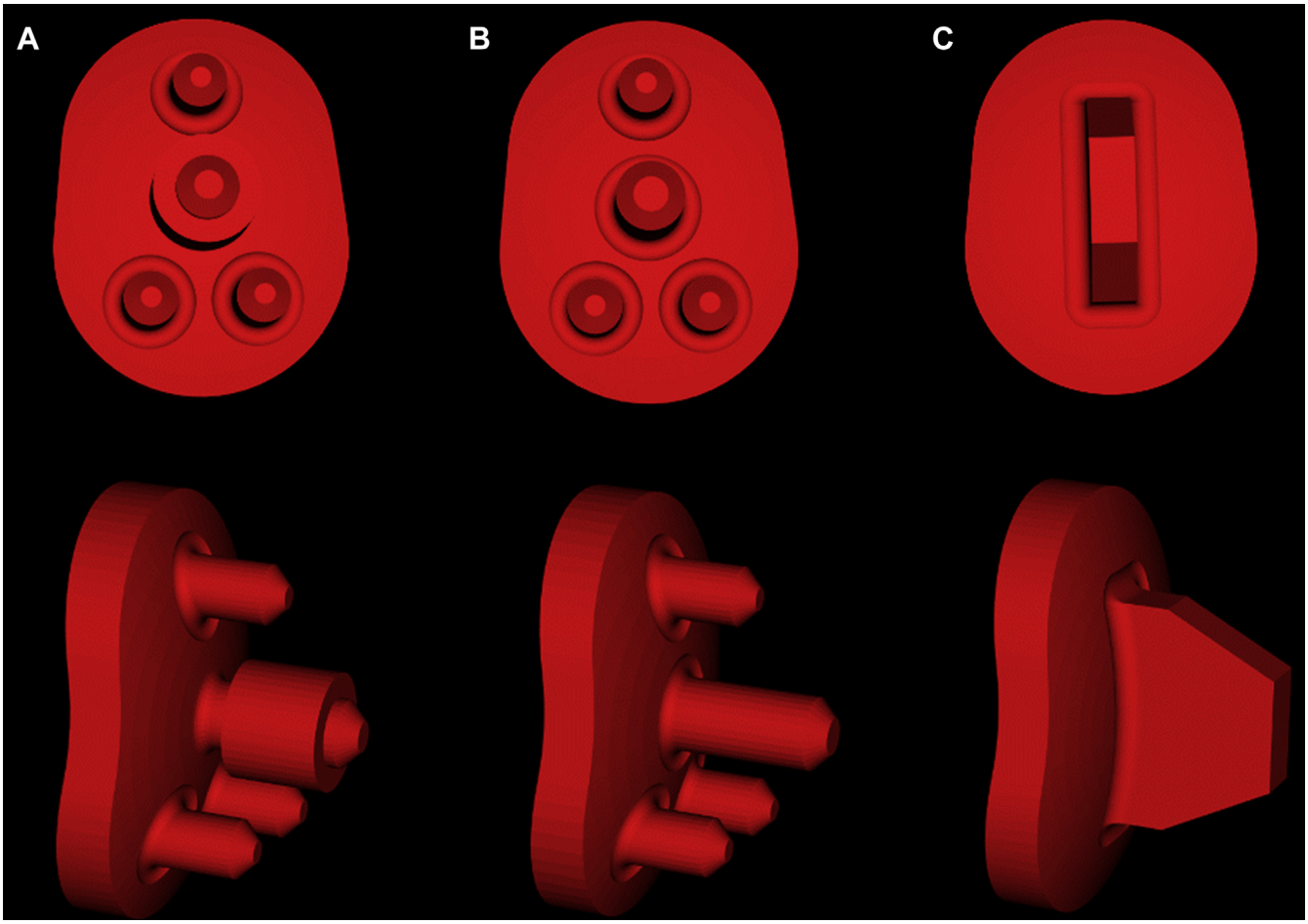

Figure 1 Three-dimensional surfaces for the Wright Tornier Aequalis Perform Glenoid System including the (**A**) Cortiloc, (**B**) pegged, and (**C**) keeled fixation types.

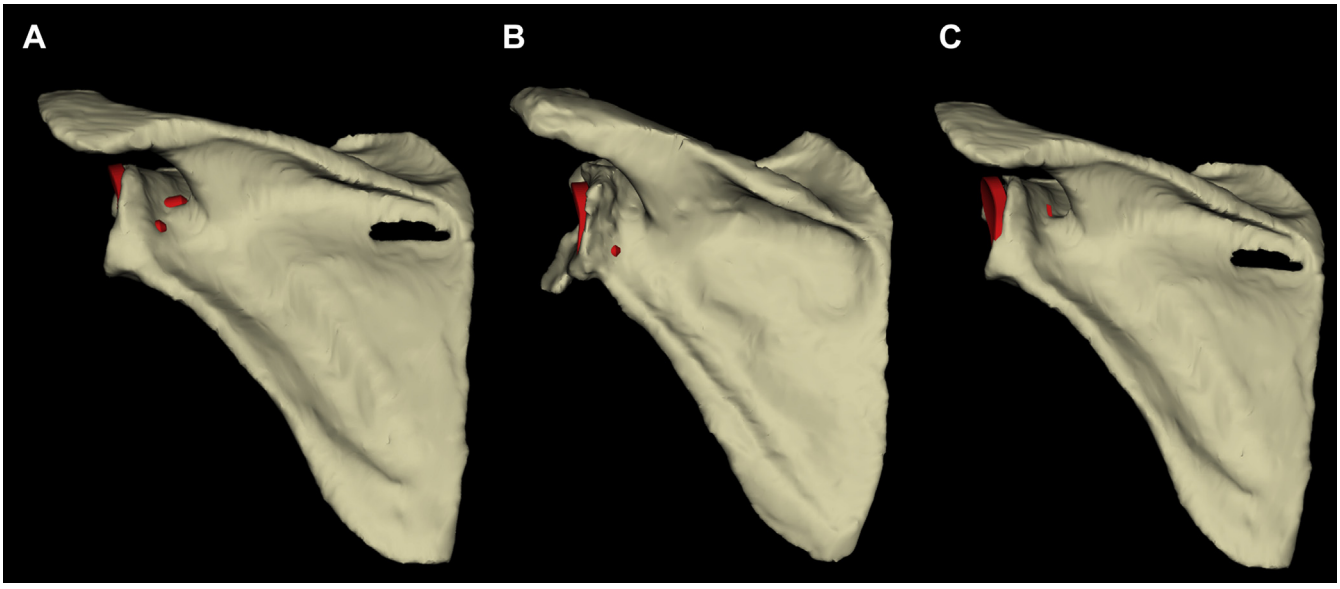

Figure 2 Representative examples of implant perforation of the glenoid vault visualized using the Tornier BluePrint v2.1.5 software and the (**A**) Cortiloc, (**B**) pegged, and (**C**) keeled implants.

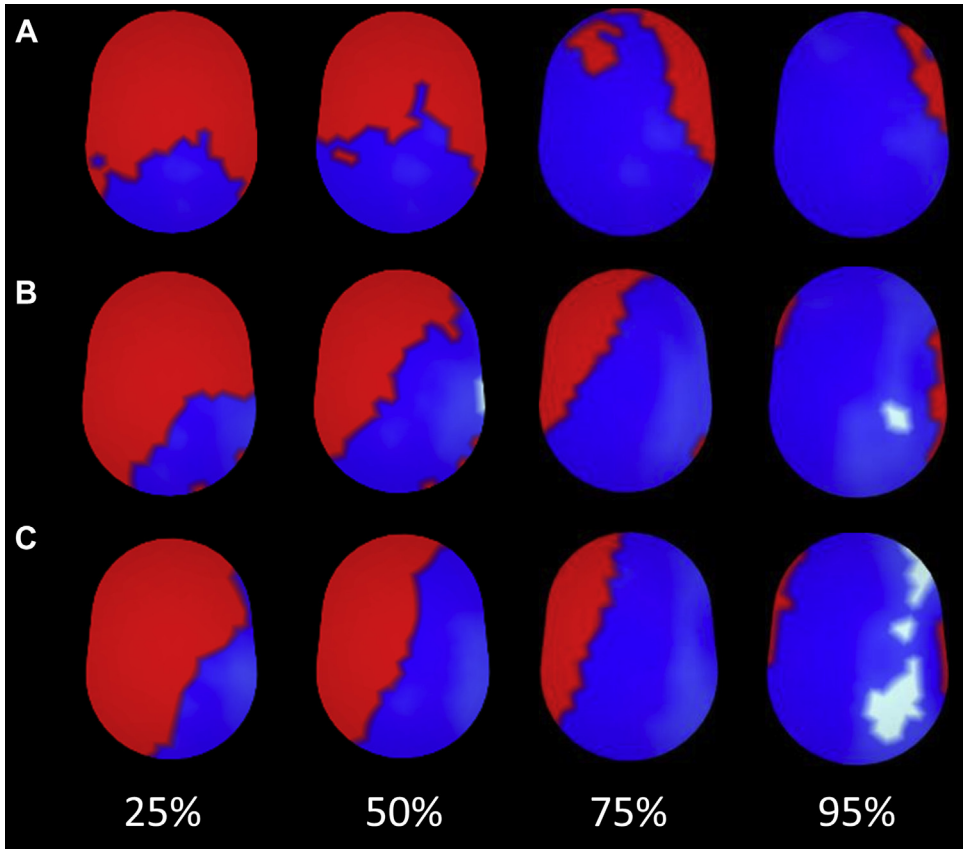

Figure 3 Representative color maps from a single subject demonstrating contact of the implant base with the glenoid surface, where *red* indicates no contact; *blue*, cortical contact; and *white*, cancellous contact. Represented here are bone-implant contact area percentages of 25%, 50%, 75%, and 95% for (**A**) scenario 1, (**B**) scenario 2, and (**C**) scenario 3.

Table I Medialization distance and standard deviation of the Cortiloc implant based on scenario and implant seating percentage

Scenario	Seating percentage	Medialization, mm	Standard deviation, mm
1	25	−1.00	0.55
	50	0.00	0.52
	75	0.50	0.52
	95	1.00	0.63
2	25	−2.00	0.89
	50	0.00	0.42
	75	1.25	1.16
	95	3.00	2.07
3	25	−2.50	0.96
	50	0.00	0.52
	75	2.50	1.39
	95	5.00	2.13

Table II Medialization distance and standard deviation of the pegged implant based on scenario and implant seating percentage

Scenario	Seating percentage	Medialization, mm	Standard deviation, mm
1	25	−1.00	0.56
	50	−0.25	0.52
	75	0.50	0.27
	95	1.00	0.63
2	25	−2.00	0.87
	50	0.00	0.45
	75	1.00	1.17
	95	2.50	1.98
3	25	−2.50	0.97
	50	0.00	0.52
	75	2.50	1.40
	95	5.00	2.51

required to achieve 75% contact was 0.5, 1.25, and 2.50 mm for scenarios 1, 2, and 3, respectively.

The BICA maps were visually inspected for all simulated cases (Fig. 3). We noted that with correction of glenoid retroversion, 75% of BICA is required for the posterior portion of the implant to contact the glenoid. In the cases of glenoid deformity correction, the contact interface progressed posteriorly from anteroinferior coverage with increasing amounts of medialization and higher levels of BICA. In the case without glenoid deformity correction, the contact interface was more balanced in the anterior-posterior direction.

Table III Medialization distance and standard deviation of the keeled implant based on scenario and implant seating percentage

Scenario	Seating percentage	Medialization, mm	Standard deviation, mm
1	25	−1.00	0.64
	50	0.00	0.53
	75	0.50	0.52
	95	1.00	0.63
2	25	−2.00	1.00
	50	0.00	0.43
	75	1.50	1.21
	95	3.00	1.98
3	25	−2.50	0.97
	50	0.00	0.55
	75	2.50	1.40
	95	5.00	2.14

Across all scenarios, the incidence of perforation increased with increasing medialization distance and implant-bone contact percentage. Overall, the Cortiloc implant was most likely to perforate the glenoid vault, and the keeled implant was least likely to perforate the glenoid vault (Figs. 4-6). With regard to implant fixation type, the central and posterior-inferior pegs were most likely to perforate across all simulations for the Cortiloc and pegged designs (Figs. 7-9).

In the case without glenoid deformity correction, the Cortiloc implant had a 10%-14% chance of perforation for a 75%-95% implant seating (Fig. 10). Partial correction of the glenoid version resulted in a 26%-42% chance of perforation for a 75%-95% implant seating, whereas complete correction of the glenoid version resulted in a 54%-68% chance of perforation for a 75%-95% implant seating. Complete correction of glenoid version and inclination nearly doubled the perforation risk seen with partial correction using the Cortiloc implant.

In the case of no glenoid deformity correction, the pegged implant had 6%-12% chance of perforation for a 75%-95% implant seating (Fig. 11). Partial correction of the glenoid version resulted in a 20%-36% chance of perforation for a 75%-95% implant seating. Complete correction of the glenoid version results in a 40%-64% chance of perforation for a 75%-95% implant seating. Complete correction of glenoid version and inclination nearly doubled the perforation risk seen with partial correction using the pegged implant.

In the case without glenoid deformity correction, the keeled implant had a 0%-2% chance of perforation for a 75%-95% implant seating (Fig. 12). Partial correction of the glenoid version resulted in a 6%-8% chance of perforation for a 75%-95% implant seating. Complete correction of the glenoid version results in a 26%-28% chance of perforation for a 75%-95% implant seating. Complete correction of glenoid version and inclination nearly quadruples the perforation risk seen with partial correction using the keeled implant.

Discussion

In this study, we have evaluated the relationship of variable degree correction of modified Walch B/C-type glenoid morphology with eccentric reaming and the risk of glenoid vault perforation with 3 implant fixation designs. Compared with a partial correction of retroversion, complete deformity correction to neutral version via eccentric reaming increases the risk of implant perforation at high degrees (>75% contact area) of implant seating. Increased medialization distance during eccentric reaming results in increased incidence of vault perforation regardless of the implant fixation type. Although this trend was common for all components, the frequency of perforation did vary by implant type. The Cortiloc implant was associated with the highest perforation risk followed by the pegged design, and lastly the keeled fixation design.

Like others have reported, eccentric reaming in cases of complex glenoid deformity increases the likelihood of the glenoid component perforating the vault.[14,21] A keeled implant decreases risk of vault perforation when extensive reaming is used to correct glenoid deformity. Hoenecke et al[18] conducted a cadaveric study with 40 shoulder CTs and preoperative templating software and found that keeled components perforated the vault in 13% cases compared with 18% with a standard peg model and 8% with a modified peg model.[14] We observed a similar trend in our study, with components requiring less bone stock decreasing the incidence of vault perforation. The keeled component had the lowest risk of vault perforation, and the pegged design, with the smaller central peg, had fewer perforations compared with the Cortiloc (Figs. 7-9).

Clavert et al[8] simulated 5 cases of correcting 15°-31° of retroversion to neutral on cadaveric models, and in each case 1 of the 4 pegs of the glenoid component perforated the vault. In our analysis, with complete correction (scenario 3) and 75% BICA, the Cortiloc implant perforated 52% of cases, pegged implant perforated 39% of cases, and the keeled implant perforated 24% of cases. The advantage of this 3-dimensional surgical planning study compared with a cadaveric study is the number of simulations that were performed; this would have been prohibitive in a cadaveric study. Furthermore, incorporation of 3-dimensional imaging allows for optimization of implant position to allow for the ideal placement of the implant in the glenoid vault for perforation analysis, which is not possible in a cadaveric model.

Poor implant positioning, residual retroversion, posterior instability, and excessive reaming can lead to early implant loosening.[1] The long-term effects of anatomic TSA implant vault perforation on clinical outcomes and implant stability is unclear.[20,35] Press et al showed no significant relationship between incidence of perforation and number of perforations and radiolucency scores.[23] They found that both the perforation group and the control group had significant

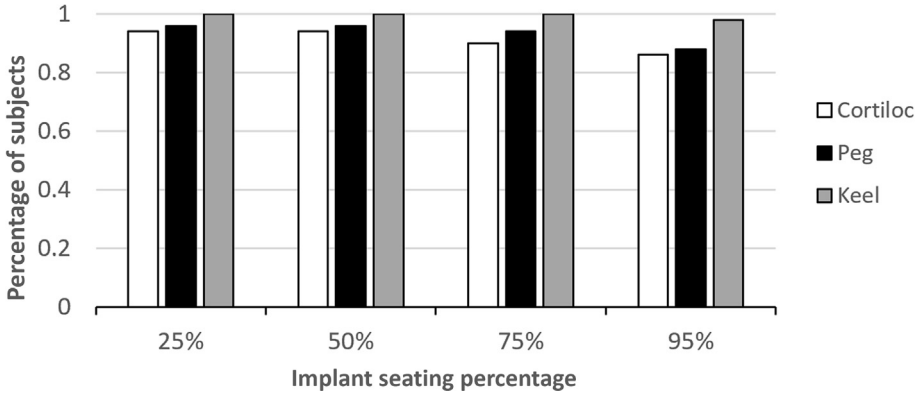

Figure 4 Graph demonstrating the percentage of subjects without glenoid perforation based on implant and bone-implant contact area percentage for scenario 1.

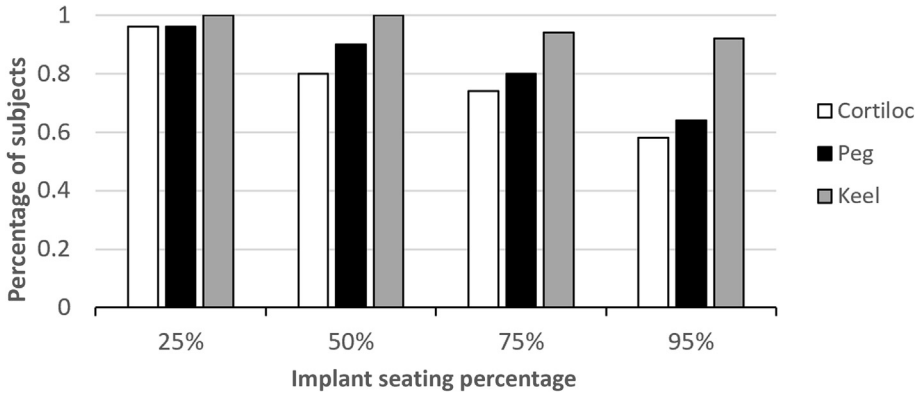

Figure 5 Graph demonstrating the percentage of subjects without glenoid perforation based on implant and bone-implant contact area percentage for scenario 2.

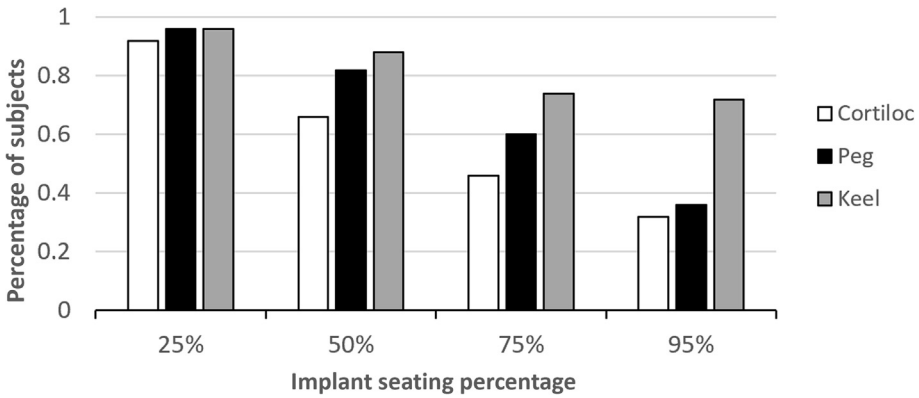

Figure 6 Graph demonstrating the percentage of subjects without glenoid perforation based on implant and bone-implant contact area percentage for scenario 3.

improvements in outcome scores. Hsu et al[17] conducted a study that assessed outcomes of uncontained pegs at 5-year follow-up and found no relationship to component loosening and no significant difference in pain or satisfaction between groups, but function was found to be significantly worse in the uncontained peg group. Further studies with larger sample sizes and longer follow-up are necessary to clarify the impact of implant perforation of the glenoid vault.

Previous studies have shown that residual retroversion after deformity correction can place the glenoid component at a biomechanical disadvantage and be a risk factor for loosening.[11] Farron et al[11] recommend leaving no more than 10° of retroversion. Eccentric reaming for glenoid deformity correction reduces vault bone stock as a result of medialization, which we hypothesized would increase the risk for vault perforation. We found that with increased

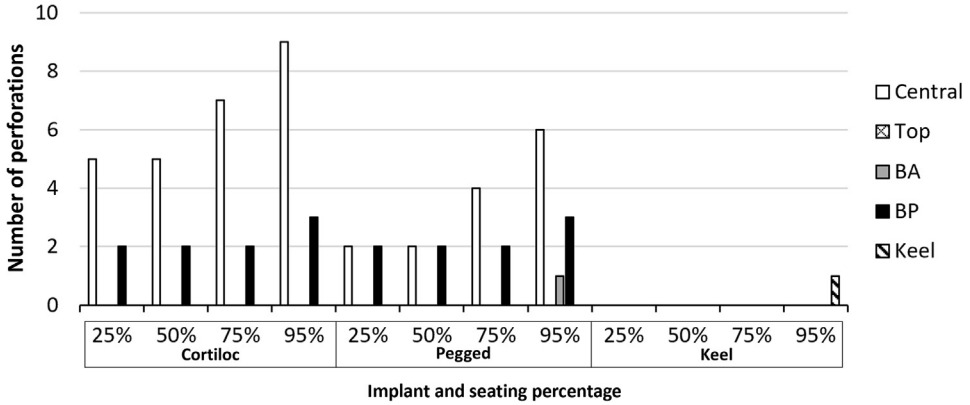

Figure 7 Graph depicting the total number of perforations based on implant, bone-implant contact area percentage, and portion of implant that perforated for scenario 1.

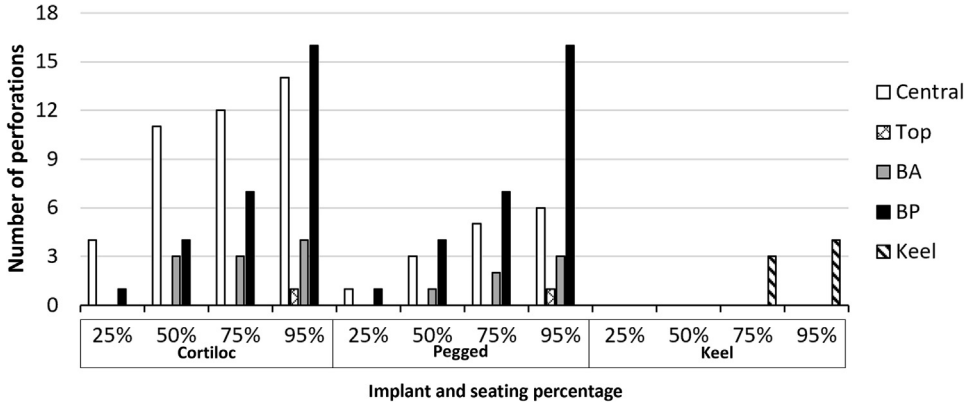

Figure 8 Graph depicting the total number of perforations based on implant, bone-implant contact area percentage, and portion of implant that perforated for scenario 2.

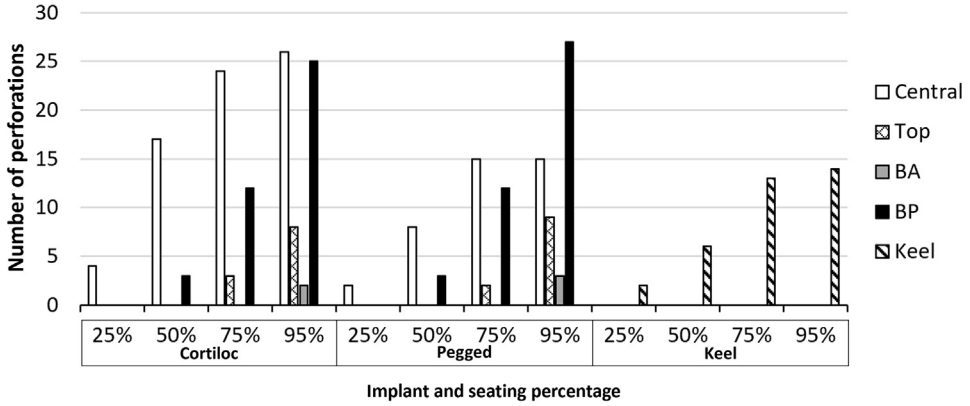

Figure 9 Graph depicting the total number of perforations based on implant, bone-implant contact area percentage, and portion of implant that perforated for scenario 3.

reaming, the risk of perforation increased. Partial correction of glenoid deformities may offer a balance of deformity correction and reduced vault perforation compared with complete glenoid deformity correction.

Walch et al[48] performed a clinical outcomes study on eccentric reaming in 108 anatomic TSA patients with biconcave glenoids from 1991-2007 with an average follow-up of 77 months. They used 2D measurements on CT imaging to determine if it was possible to eccentrically ream the anterior glenoid to achieve a final retroversion between 0°-10°. If this was not possible, they performed structural bone grafting. Overall, they report acceptable clinical outcomes but a high rate of complications, including glenoid loosening (20.6%), which was associated

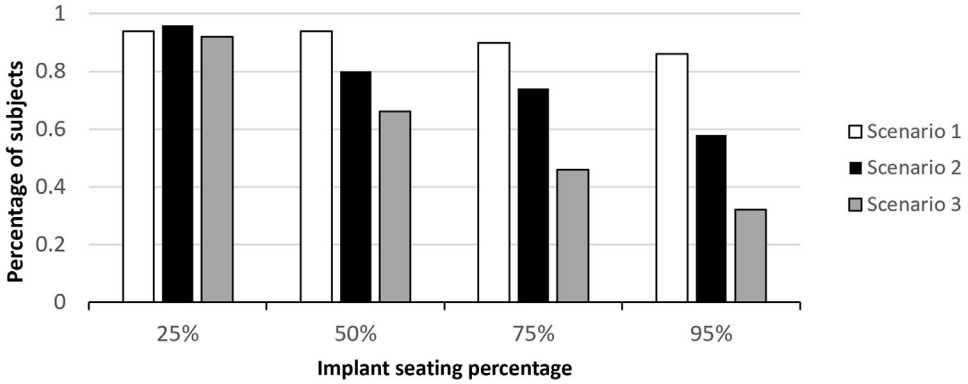

Figure 10 Graph demonstrating the percentage of subjects without glenoid perforation based on reaming scenario and bone-implant contact area percentage for the Cortiloc implant.

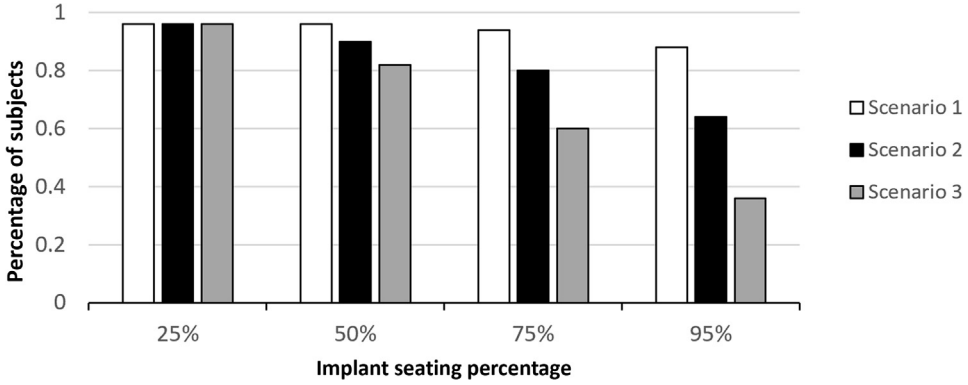

Figure 11 Graph demonstrating the percentage of subjects without glenoid perforation based on reaming scenario and bone-implant contact area percentage for the pegged implant.

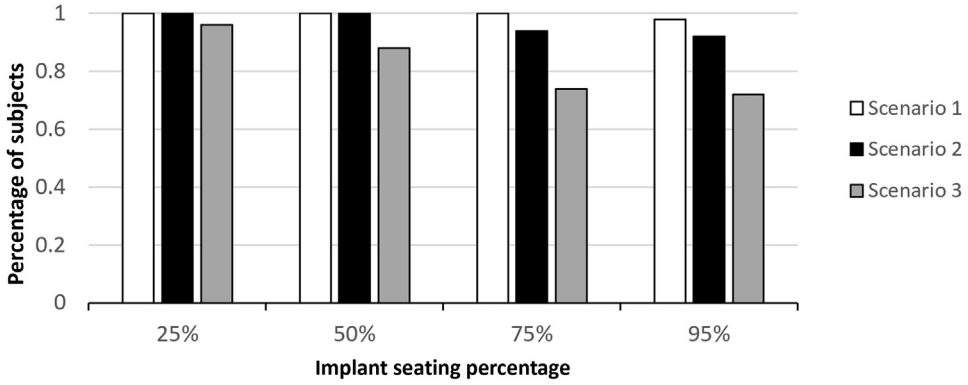

Figure 12 Graph demonstrating the percentage of subjects without glenoid perforation based on reaming scenario and bone-implant contact area seating percentage for the keeled implant.

with increased amounts of posterior erosion, posterior humeral subluxation, and retroversion. In this study, we use modern 3D modeling tools to optimize glenoid implant positioning in the case of complex glenoid deformity. Future studies using this toolset may offer a method to improve upon these previously reported results.

With regard to implant fixation type, the keeled design consists of a single component that is designed to stay centrally located within the glenoid vault. The other fixation types that we evaluated included peripheral pegs and widened central pegs that required larger amounts of bone stock to be contained. We have demonstrated that the keeled fixation design consistently had the lowest perforation risk and may offer versatility in balancing vault containment with eccentric reaming for complex glenoid morphology correction.

In this study, we have only evaluated a single implant system. We selected the Wright Tornier Aequalis Perform

Glenoid System to ensure compatibility with the selected preoperative planning software. Additionally, we did not evaluate augmented glenoid implants[2,42,45] or structural bone grafting[16,26] as other options to manage complex glenoid morphology. We had hypothesized that a glenoid BICA of 75% is sufficient for anatomic TSA. Finite element studies have investigated implant contact stresses in anatomic TSA, but the minimal required BICA value has not been reported.[51] In reverse TSA, it is recommended that at least 80% of the glenosphere baseplate be in contact with bone.[25,27-29] This study evaluated implant positioning but did not evaluate the effects of soft tissue considerations (posterior plication and releases), which can affect wear patterns, stability, and joint mechanics of anatomic TSA implants.

Conclusion

Partial correction of modified Walch B/C-type glenoid deformity with eccentric reaming can achieve acceptable implant position and 75% BICA while reducing the risk of vault perforation compared with complete correction to neutral inclination and version. Keeled components had the lowest risk of vault perforation and may offer versatility in balancing vault containment with eccentric reaming and complex glenoid morphology correction.

Acknowledgments

The authors thank M. Tyrell Burrus, MD for his contributions to the early study design of this project.

Disclaimer

Michael Freehill reports being a consultant and receiving research support for Smith & Nephew and a consultant for Integra.

Jon Warner reports royalty and consulting with Wright Medical.

Asheesh Bedi reports being a consultant for Arthrex.

The other authors, their immediate families, and any research foundations with which they are affiliated have not received any financial payments or other benefits from any commercial entity related to the subject of this article.

References

1. Alentorn-Geli E, Assenmacher AT, Sperling JW, Cofield RH, Sánchez-Sotelo J. Plication of the posterior capsule for intraoperative posterior instability during anatomic total shoulder arthroplasty. J Shoulder Elbow Surg 2017;26:982-9. https://doi.org/10.1016/j.jse.2016.10.008
2. Allred JJ, Flores-Hernandez C, Hoenecke HR Jr, D'Lima DD. Posterior augmented glenoid implants require less bone removal and generate lower stresses: a finite element analysis. J Shoulder Elbow Surg 2016;25:823-30. https://doi.org/10.1016/j.jse.2015.10.003
3. Bercik MJ, Kruse K 2nd, Yalizis M, Gauci MO, Chaoui J, Walch G. A modification to the Walch classification of the glenoid in primary glenohumeral osteoarthritis using three-dimensional imaging. J Shoulder Elbow Surg 2016;25:1601-6. https://doi.org/10.1016/j.jse.2016.03.010
4. Berhouet J, Gulotta LV, Dines DM, Craig E, Warren RF, Choi D, et al. Preoperative planning for accurate glenoid component positioning in reverse shoulder arthroplasty. Orthop Traumatol Surg Res 2017;103:407-13. https://doi.org/10.1016/j.otsr.2016.12.019
5. Boileau P, Moineau G, Roussanne Y, O'Shea K. Bony increased-offset reversed shoulder arthroplasty: minimizing scapular impingement while maximizing glenoid fixation. Clin Orthop Relat Res 2011;469:2558-67. https://doi.org/10.1007/s11999-011-1775-4
6. Budge MD, Lewis GS, Schaefer E, Coquia S, Flemming DJ, Armstrong AD. Comparison of standard two-dimensional and three-dimensional corrected glenoid version measurements. J Shoulder Elbow Surg 2011;20:577-83. https://doi.org/10.1016/j.jse.2010.11.003
7. Chalmers PN, Salazar D, Chamberlain A, Keener JD. Radiographic characterization of the B2 glenoid: the effect of computed tomographic axis orientation. J Shoulder Elbow Surg 2017;26:258-64. https://doi.org/10.1016/j.jse.2016.07.021
8. Cho SW, Jharia TK, Moon YL, Sim SW, Shin DS, Bigliani LU. Three-dimensional templating arthroplasty of the humeral head. Surg Radiol Anat 2013;35:685-8. https://doi.org/10.1007/s00276-013-1090-8
9. Dallalana RJ, McMahon RA, East B, Geraghty L. Accuracy of patient-specific instrumentation in anatomic and reverse total shoulder arthroplasty. Int J Shoulder Surg 2016;10:59-66. https://doi.org/10.4103/0973-6042.180717
10. Ernstbrunner L, Werthel JD, Wagner E, Hatta T, Sperling JW, Cofield RH. Glenoid bone grafting in primary reverse total shoulder arthroplasty. J Shoulder Elbow Surg 2017;26:1441-7. https://doi.org/10.1016/j.jse.2017.01.011
11. Farron A, Terrier A, Buchler P. Risks of loosening of a prosthetic glenoid implanted in retroversion. J Shoulder Elbow Surg 2006;15:521-6. https://doi.org/10.1016/j.jse.2005.10.003
12. Gauci MO, Boileau P, Baba M, Chaoui J, Walch G. Patient-specific glenoid guides provide accuracy and reproducibility in total shoulder arthroplasty. Bone Joint J 2016;98-B:1080-5. https://doi.org/10.1302/0301-620x.98b8.37257
13. Ghoraishian M, Abboud JA, Romeo AA, Williams GR, Namdari S. Augmented glenoid implants in anatomic total shoulder arthroplasty: review of available implants and current literature. J Shoulder Elbow Surg 2019;28:387-95. https://doi.org/10.1016/j.jse.2018.08.017
14. Gillespie R, Lyons R, Lazarus M. Eccentric reaming in total shoulder arthroplasty: a cadaveric study. Orthopedics 2009;32:21. https://doi.org/10.3928/01477447-20090101-07
15. Hermida JC, Flores-Hernandez C, Hoenecke HR, D'Lima DD. Augmented wedge-shaped glenoid component for the correction of glenoid retroversion: a finite element analysis. J Shoulder Elbow Surg 2014;23:347-54. https://doi.org/10.1016/j.jse.2013.06.008
16. Hill JM, Norris TR. Long-term results of total shoulder arthroplasty following bone-grafting of the glenoid. J Bone Joint Surg Am 2001;83:877-83.
17. Ho JC, Sabesan VJ, Iannotti JP. Glenoid component retroversion is associated with osteolysis. J Bone Joint Surg Am 2013;95:e82. https://doi.org/10.2106/jbjs.L.00336
18. Hoenecke HR Jr, Hermida JC, Dembitsky N, Patil S, D'Lima DD. Optimizing glenoid component position using three-dimensional computed tomography reconstruction. J Shoulder Elbow Surg 2008;17:637-41. https://doi.org/10.1016/j.jse.2007.11.021
19. Hoenecke HR Jr, Tibor LM, Elias DW, Flores-Hernandez C, Steinvurzel JN, D'Lima DD. A quantitative three-dimensional templating method for shoulder arthroplasty: biomechanical validation in

cadavers. J Shoulder Elbow Surg 2012;21:1377-83. https://doi.org/10.1016/j.jse.2011.10.011
20. Hsu JE, Hackett DJ Jr, Vo KV, Matsen FA 3rd. What can be learned from an analysis of 215 glenoid component failures? J Shoulder Elbow Surg 2018;27:478-86. https://doi.org/10.1016/j.jse.2017.09.029
21. Iannotti JP, Greeson C, Downing D, Sabesan V, Bryan JA. Effect of glenoid deformity on glenoid component placement in primary shoulder arthroplasty. J Shoulder Elbow Surg 2012;21:48-55. https://doi.org/10.1016/j.jse.2011.02.011
22. Iannotti JP, Weiner S, Rodriguez E, Subhas N, Patterson TE, Jun BJ, et al. Three-dimensional imaging and templating improve glenoid implant positioning. J Bone Joint Surg Am 2015;97:651-8. https://doi.org/10.2106/jbjs.N.00493
23. Jones RB. Addressing glenoid erosion in anatomic total shoulder arthroplasty. Bull Hosp Jt Dis (2013) 2013;71(Suppl 2):S46-50.
24. Jones RB, Wright TW, Roche CP. Bone grafting the glenoid versus use of augmented glenoid baseplates with reverse shoulder arthroplasty. Bull Hosp Jt Dis (2013) 2015;73(Suppl 1):S129-35.
25. Klein SM, Dunning P, Mulieri P, Pupello D, Downes K, Frankle MA. Effects of acquired glenoid bone defects on surgical technique and clinical outcomes in reverse shoulder arthroplasty. J Bone Joint Surg Am 2010;92:1144-54. https://doi.org/10.2106/jbjs.i.00778
26. Klika BJ, Wooten CW, Sperling JW, Steinmann SP, Schleck CD, Harmsen WS, et al. Structural bone grafting for glenoid deficiency in primary total shoulder arthroplasty. J Shoulder Elbow Surg 2014;23:1066-72. https://doi.org/10.1016/j.jse.2013.09.017
27. Lorenzetti A, Streit JJ, Cabezas AF, Christmas KN, LaMartina J 2nd, Simon P, et al. Bone graft augmentation for severe glenoid bone loss in primary reverse total shoulder arthroplasty: outcomes and evaluation of host bone contact by 2D-3D image registration. JB JS Open Access 2017;2:e0015. https://doi.org/10.2106/jbjs.oa.17.00015
28. Malhas A, Rashid A, Copas D, Bale S, Trail I. Glenoid bone loss in primary and revision shoulder arthroplasty. Shoulder Elbow 2016;8:229-40. https://doi.org/10.1177/1758573216648601
29. Matache BA, Lapner P. Anatomic shoulder arthroplasty: technical considerations. Open Orthop J 2017;11:1115-25. https://doi.org/10.2174/1874325001711011115
30. McFarland EG, Huri G, Hyun YS, Petersen SA, Srikumaran U. Reverse total shoulder arthroplasty without bone-grafting for severe glenoid bone loss in patients with osteoarthritis and intact rotator cuff. J Bone Joint Surg Am 2016;98:1801-7. https://doi.org/10.2106/jbjs.15.01181
31. Mizuno N, Denard PJ, Raiss P, Walch G. Reverse total shoulder arthroplasty for primary glenohumeral osteoarthritis in patients with a biconcave glenoid. J Bone Joint Surg Am 2013;95:1297-304. https://doi.org/10.2106/jbjs.l.00820
32. Nowak DD, Bahu MJ, Gardner TR, Dyrszka MD, Levine WN, Bigliani LU, et al. Simulation of surgical glenoid resurfacing using three-dimensional computed tomography of the arthritic glenohumeral joint: the amount of glenoid retroversion that can be corrected. J Shoulder Elbow Surg 2009;18:680-8. https://doi.org/10.1016/j.jse.2009.03.019
33. Obert L, Peyron C, Boyer E, Menu G, Loisel F, Aubry S. CT scan evaluation of glenoid bone and pectoralis major tendon: interest in shoulder prosthesis. SICOT J 2016;2:33. https://doi.org/10.1051/sicotj/2016021
34. Osmani FA, Thakkar S, Ramme A, Elbuluk A, Wojack P, Vigdorchik JM. Variance in predicted cup size by 2-dimensional vs 3-dimensional computerized tomography-based templating in primary total hip arthroplasty. Arthroplast Today 2017;3:289-93. https://doi.org/10.1016/j.artd.2016.09.003
35. Press CM, O'Connor DP, Elkousy HA, Gartsman GM, Edwards TB. Glenoid perforation does not affect the short-term outcomes of pegged all-polyethylene implants in total shoulder arthroplasty. J Shoulder Elbow Surg 2014;23:1203-7. https://doi.org/10.1016/j.jse.2013.11.024
36. Ramme AJ, Egol J, Chang G, Davidovitch RI, Konda S. Evaluation of malrotation following intramedullary nailing in a femoral shaft fracture model: can a 3D c-arm improve accuracy? Injury 2017;48:1603-8. https://doi.org/10.1016/j.injury.2017.03.041
37. Ramme AJ, Fisher ND, Egol J, Chang G, Vigdorchik JM. Scaling marker position determines the accuracy of digital templating for total hip arthroplasty. HSS J 2018;14:55-9. https://doi.org/10.1007/s11420-017-9578-0
38. Ramme AJ, Iorio R, Smiaronksi J, Wronka A, Rodriguez G, Specht L, et al. Organizational and technical considerations for the implementation of a digital orthopaedic templating system. Bull Hosp Jt Dis (2013) 2016;74:254-61.
39. Ramme AJ, Wolf BR, Warme BA, Shivanna KH, Willey MC, Britton CL, et al. Surgically oriented measurements for three-dimensional characterization of tunnel placement in anterior cruciate ligament reconstruction. Comput Aided Surg 2012;17:221-31. https://doi.org/10.3109/10929088.2012.707230
40. Sabesan V, Callanan M, Sharma V, Iannotti JP. Correction of acquired glenoid bone loss in osteoarthritis with a standard versus an augmented glenoid component. J Shoulder Elbow Surg 2014;23:964-73. https://doi.org/10.1016/j.jse.2013.09.019
41. Sabesan VJ, Lima DJL, Whaley JD, Pathak V, Zhang L. Biomechanical comparison of 2 augmented glenoid designs: an integrated kinematic finite element analysis. J Shoulder Elbow Surg 2019;28:1166-74. https://doi.org/10.1016/j.jse.2018.11.055
42. Sandow M, Schutz C. Total shoulder arthroplasty using trabecular metal augments to address glenoid retroversion: the preliminary result of 10 patients with minimum 2-year follow-up. J Shoulder Elbow Surg 2016;25:598-607. https://doi.org/10.1016/j.jse.2016.01.001
43. Sears BW, Johnston PS, Ramsey ML, Williams GR. Glenoid bone loss in primary total shoulder arthroplasty: evaluation and management. J Am Acad Orthop Surg 2012;20:604-13. https://doi.org/10.5435/jaaos-20-09-604
44. Stephens SP, Paisley KC, Jeng J, Dutta AK, Wirth MA. Shoulder arthroplasty in the presence of posterior glenoid bone loss. J Bone Joint Surg Am 2015;97:251-9. https://doi.org/10.2106/jbjs.N.00566
45. Stephens SP, Spencer EE, Wirth MA. Radiographic results of augmented all-polyethylene glenoids in the presence of posterior glenoid bone loss during total shoulder arthroplasty. J Shoulder Elbow Surg 2017;26:798-803. https://doi.org/10.1016/j.jse.2016.09.053
46. Strauss EJ, Roche C, Flurin PH, Wright T, Zuckerman JD. The glenoid in shoulder arthroplasty. J Shoulder Elbow Surg 2009;18:819-33. https://doi.org/10.1016/j.jse.2009.05.008
47. Ting FS, Poon PC. Perforation tolerance of glenoid implants to abnormal glenoid retroversion, anteversion, and medialization. J Shoulder Elbow Surg 2013;22:188-96. https://doi.org/10.1016/j.jse.2011.12.009
48. Walch G, Moraga C, Young A, Castellanos-Rosas J. Results of anatomic nonconstrained prosthesis in primary osteoarthritis with biconcave glenoid. J Shoulder Elbow Surg 2012;21:1526-33. https://doi.org/10.1016/j.jse.2011.11.030
49. Walch G, Vezeridis PS, Boileau P, Deransart P, Chaoui J. Three-dimensional planning and use of patient-specific guides improve glenoid component position: an in vitro study. J Shoulder Elbow Surg 2015;24:302-9. https://doi.org/10.1016/j.jse.2014.05.029
50. Wang T, Abrams GD, Behn AW, Lindsey D, Giori N, Cheung EV. Posterior glenoid wear in total shoulder arthroplasty: eccentric anterior reaming is superior to posterior augment. Clin Orthop Relat Res 2015;473:3928-36. https://doi.org/10.1007/s11999-015-4482-8
51. Wee H, Armstrong AD, Flint WW, Kunselman AR, Lewis GS. Peri-implant stress correlates with bone and cement morphology: micro-FE modeling of implanted cadaveric glenoids. J Orthop Res 2015;33:1671-9. https://doi.org/10.1002/jor.22933
52. Werner BS, Hudek R, Burkhart KJ, Gohlke F. The influence of three-dimensional planning on decision-making in total shoulder arthroplasty. J Shoulder Elbow Surg 2017;26:1477-83. https://doi.org/10.1016/j.jse.2017.01.006